Environmental Science and Pollution Research (2020) 27:27048–27060
https://doi.org/10.1007/s11356-020-09053-z

RESEARCH ARTICLE

Caffeine removal using *Elaeis guineensis* activated carbon: adsorption and RSM studies

Larissa L. A. Melo[1] · Alessandra H. Ide[1] · José Leandro S. Duarte[1,2] · Carmem Lucia P. S. Zanta[2] · Leonardo M. T. M. Oliveira[1] · Wagner R. O. Pimentel[1] · Lucas Meili[1]

Received: 18 November 2019 / Accepted: 27 April 2020 / Published online: 9 May 2020

Abstract

The palm (*Elaeis guineensis*), known as *dendê*, is an important oleaginous Brazilian plant with a high performance of oil production. In this work, a 2^3 full experimental design was performed and the response surface method (RSM) was used to indicate the optimum parameter of caffeine adsorption on *Elaeis guineensis* endocarp activated carbon, since the endocarp is the main by-product from *dendê* oil production. It was set the adsorbent point of zero charge (pH_{pzc}), and the material was characterized by Fourier transform infrared spectroscopy (FT-IR), thermogravimetric analysis (TGA), and scanning electron microscopy (SEM). The RSM results indicate removal efficiency (%) at the optimal conditions, 0.20 g of adsorbent, and caffeine initial concentration of 20 mg/L, and acidic medium was about 95%. Based on ANOVA and *F* test ($F_{calculated} > F_{standard}$), the mathematical/statistical model obtained fits well to the experimental data. The overall kinetic studies showed time was achieved after 5 h and caffeine adsorption followed the pseudo-second-order model suggesting chemisorption is a predominant mechanism. Redlich-Peterson and Sips models best represented the experimental data ($0.967 < R^2 < 0.993$). Thermodynamic revealed that caffeine adsorption was spontaneous at all temperatures studied, exothermic, and probably with changes in the adsorbate-adsorbent complex during the process. The tests conducted in different water matrixes corroborate the suitability of this adsorbent to be used in caffeine removal even in a complex solution.

Keywords Pharmaceuticals · Biochar · Emerging pollutants · Wastewater

Introduction

Caffeine is a weak alkaloid of the methylxanthine family, 1,3,7-timetylxanthine. This substance is classified as a drug, is a nervous system stimulant, and causes transient changes in blood pressure. Caffeine is used as an adjuvant in many pharmaceutical combinations to increase its analgesic effects. It is present in beverages such as coffee, teas, chocolates, and soft drinks. The metabolism of this substance is rapid where only a small amount (1–10%) is excreted (Thorn et al. 2012; Portinho et al. 2017; Beltrame et al. 2018; Ptaszkowska-Koniarz et al. 2018; Yamamoto et al. 2018; González et al. 2019). Many pharmaceutical compounds, such as caffeine, are considered water contaminants and classified as emerging pollutants. This class of pollutants now attracted attention as an environmental problem due to its presence that had been recently detected in the environment. Several researchers consider caffeine as an indicator substance of human pollution due its resilience to conventional water and wastewater treatments. Therefore, this substance has often been found in surface water and groundwater (Álvarez-Torrellas et al. 2017; Portinho et al. 2017; Wang et al. 2017; Beltrame et al. 2018).

Many methods can be used to reduce caffeine concentration in water. Among these methods, adsorption stands out due to its simplicity of design and operation, minimal energy requirements, possibility of adsorbent regeneration, and no generation of dangerous by-products (Álvarez-Torrellas et al. 2017). The wide range of materials to be used as adsorbents is one of the great advantages of adsorption. This characteristic

Responsible editor: Tito Roberto Cadaval Jr

✉ Lucas Meili
lucas.meili@ctec.ufal.br

[1] Laboratório de Processos, Centro de Tecnologia, Universidade Federal de Alagoas, Av. Lourival Melo Mota, Tabuleiro dos Martins, Maceió, AL 57072-970, Brazil

[2] Laboratorio de Eletroquímica Aplicada, Instituto de Química e Biotecnologia, Universidade Federal de Alagoas, Av. Lourival Melo Mota, Tabuleiro dos Martins, Maceió, AL 57072-970, Brazil

makes this technique still of great interest, especially in the search for materials with high efficiency of adsorption, low production costs, and high capacity of regeneration.

In order to conduct an efficient evaluation of DS removal and to maximize the adsorption yield, an optimization study should be developed (Wakkel et al. 2019). The response surface methodology (RSM) is a combination of statistical and mathematical techniques which allow investigating the effect of several independent variables. This approach enables to obtain empirical models and to design, improve, and optimize several types of processes. The use of RSM, a multivariate optimization technique, is convenient once it employs experimental data and permits to evaluate the interactive effect of variables on process performance. Thus, RSM overcomes situations requiring a large number of experiments minimizing additional chemicals, time, and expensive analysis, promoting a reduction of extra costs (Biswas et al. 2019; Şahan 2019). RSM advantages guaranteed its application in several works regarding the removal of contaminants from water to process parameter optimization, such as adsorption (Kaynar et al. 2018; Biswas et al. 2019; Deng and Chen 2019; Hasan and Setiabudi 2019; Kaur et al. 2019; Şahan 2019; Sharifpour et al. 2019; Wakkel et al. 2019), electrocoagulation (Barsç and Turkay 2016; Murdani et al. 2018; Rabahi et al. 2018; Deveci et al. 2019; Karamati-Niaragh et al. 2019), Fenton reaction (Saeed et al. 2015; Xie et al. 2016; Liu et al. 2018), electrochemical oxidation (Garg and Prasad 2015; Domínguez et al. 2016; Darvishmotevalli et al. 2019; Duarte et al. 2019), and photocatalytic degradation (Mirzaei et al. 2018; Galedari et al. 2019; Karimi et al. 2019).

Activated carbons are among the most used materials as adsorbent. Recently, several researches have been conducted to obtain new activated carbons from renewable sources, such as agroindustry by-products (Suzuki et al. 2007; Beltrame et al. 2018), papaya seeds (Weber et al. 2013), *Syagrus oleracea* endocarp (dos Santos et al. 2019a), *Wodyetia bifurcata* endocarp (dos Santos et al. 2019b), coconut shells (Chandana et al. 2019), rice husks (Lv et al. 2020), wood sawmills (Ramirez et al. 2020), and apple seed shells (Abatan et al. 2019). The palm (*Elaeis guineensis*), known as *dendê*, is a typical Brazilian palm tree that is the higher oil producer per unit of cultivated area among other oleaginous plants in Brazil, an average of 4–6 t of oil/ha-year (Queiroz et al. 2012) (De Azevedo et al. 2014). The palm endocarp is one of the largest by-products generated during palm oil production.

The main objective of this work was to evaluate the adsorption potential of the *Elaeis guineensis* activated carbon in the removal of the caffeine from water through batch adsorption studies. Response surface methodology (RSM) was used for the optimization of independent variables mass dosage, caffeine initial concentration, and pH to obtain the maximum caffeine removal. Kinetic, equilibrium, and thermodynamics studies were conducted to evaluate the adsorption mechanism.

Table 1 Experimental levels of independent process variables

Levels	Mass dosage (g)	Caffeine initial concentration (mg/L)	pH
− 1	0.10	20	2
0	0.15	50	6
+ 1	0.20	80	10

Materials and methods

Materials

The adsorbent used in the present study was a commercial activated carbon obtained from *Elaeis guineensis* endocarp (Pelegrini Carbon). First of all, it was triturated and sieved in order to obtain particles with a medium diameter of 337.5 nm. A stock solution of caffeine (1000 mg/L) was prepared by dissolving the analytical standard in water, which was used to prepare all the work solutions by appropriated dilution. Caffeine quantification was performed using a spectrophotometer Shimadzu UV mini-1240, with absorbance measurements at 273 nm. Calibration curve was plotted with concentrations ranging from 0.5 to 6.0 mg/L and used to determine the adsorbate concentration after all adsorption assays.

Adsorbent characterization

For the determination of the adsorbent point of zero charge (pH_{pzc}), 0.02 g of the activated carbon was added to Erlenmeyer flasks with 20 mL of NaCl 0.1 mol/L solution. The pH values were adjusted to 1.0 up to 12.0 using HCl or NaOH solutions (1.0 mol/L). The samples were stirred at 140 rpm (25 °C) for 24 h. After that, the mixtures were filtered and the final pH values were measured (Regalbuto 2006). Fourier transform infrared spectroscopy (FT-IR) was performed using a spectrophotometer Shimadzu/IRPrestige-21 through the KBr method. Spectra were obtained in the range of 4000 to 400 cm^{-1} with transmittance of 50 scans. Thermogravimetric analysis (TGA) was performed using the term scale model Shimadzu DTG-60H, in which 7 mg of the adsorbent was heated until 900 °C at the rate of 10 °C/min in an inert atmosphere (nitrogen gas) with a flow rate of 50 mL/min. The surface morphology of the adsorbent material was analyzed by the SEM Shimadzu SSX-550 model. N_2 adsorption/desorption analysis was performed in a

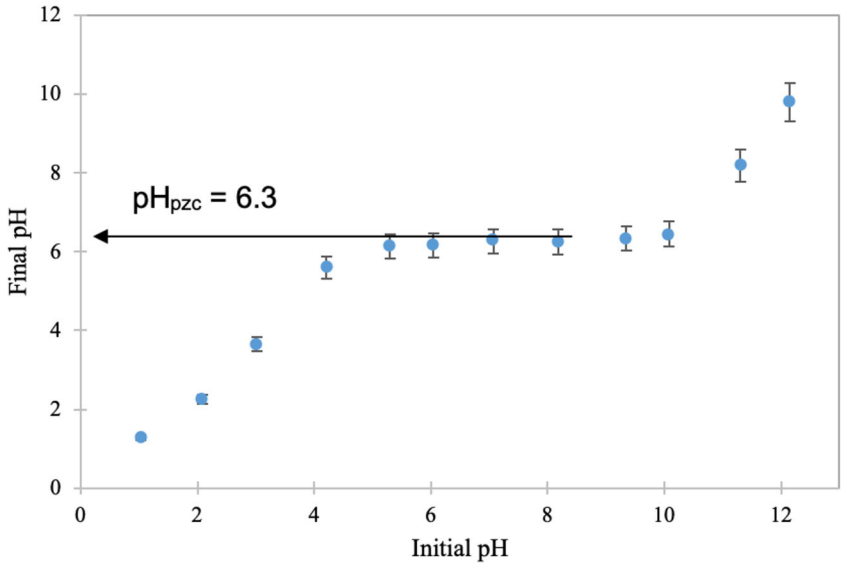

Fig. 1 Determination of pH_{pzc}

micrometrics equipment (ASAP 2020) at − 196 °C (77 K), treating the sample previously by degassing for 12 h, under vacuum (2 μm of mercury) at 350 °C, in order to remove any species on its surface. A surface external area was determined by the BET method, and the volume of pores and the distribution of their size were specified by the BJH method.

Kinetic studies

Kinetic studies were performed using a Dubnoff (SPLabor/SP-158/22/A) bath with orbital agitation. A total of 0.1 g of the adsorbent was added to Erlenmeyer flasks with 25 mL of adsorbate solution (20 mg/L) and stirred at 135 rpm (30 °C). At the end of the adsorption process, the samples were centrifuged (Solab/SL-700) at 2000 rpm for 5 min and caffeine final concentration was measured. Samples were collected at 5, 10, 15, 30, 60, 120, 180, 240, and 300 min for the construction of the kinetic curve.

In order to evaluate the adsorption capacity of the adsorbents, the adsorbed amount (q_t) in milligrams per gram and the caffeine removal (R) in percentage were calculated using Eqs. 1 and 2, respectively.

$$q_t = \frac{(C_0 - C_e)}{m} \times V \quad (1)$$

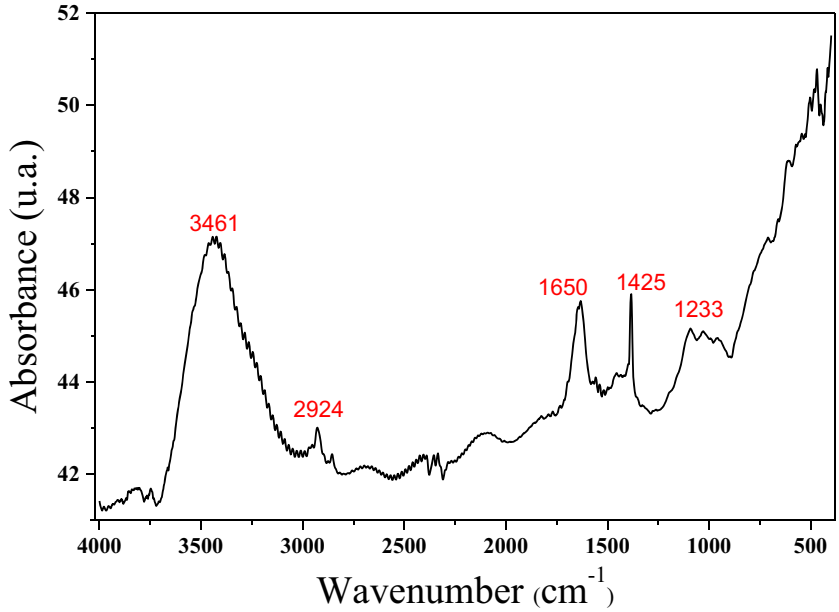

Fig. 2 Palm endocarp activated carbon FT-IR spectrum

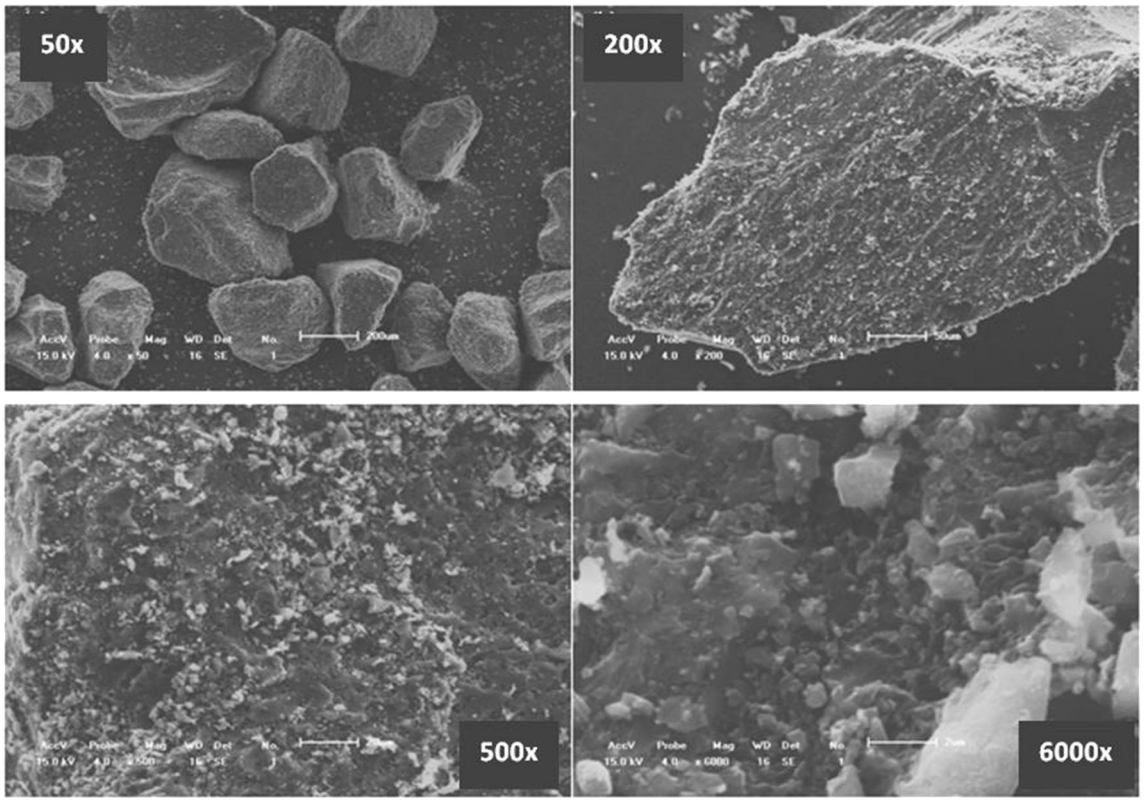

Fig. 3 SEM images of the palm endocarp activated carbon surface

$$R = \frac{C_0 - C_e}{C_0} \times 100 \quad (2)$$

where C_0 and C_e are the initial and concentration values (mg/L), respectively, m is the mass (g) of the adsorbent, and V the volume (L) of the adsorbate solution.

The experimental data were adjusted with pseudo-first-order (Eq. 3) and pseudo-second-order (Eq. 4) models (Lagergren 1898; Ho and McKay 1999).

$$q_t = q_e\left(1 - \exp^{-k_1 t}\right) \quad (3)$$

$$q_t = \frac{k_2 t {q_e}^2}{(1 + k_2 t q_e)} \quad (4)$$

where k_1 and k_2 are the first- and second-order adsorption kinetics (min^{-1} and g mg^{-1} h^{-1}), respectively, and q_t and q_e are the adsorbed adsorbent (mg g^{-1}) in equilibrium time, respectively.

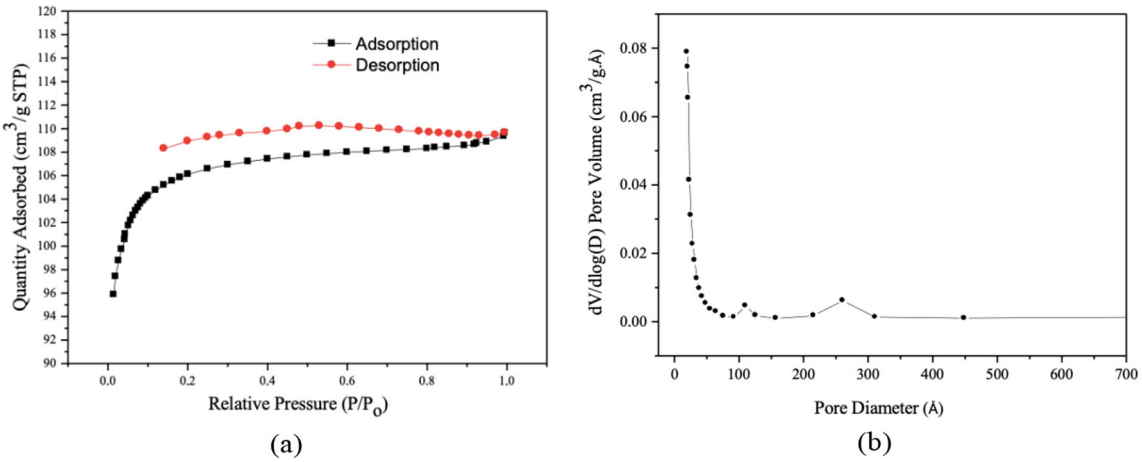

Fig. 4. **a** N_2 adsorption/desorption isotherm. **b** Pore diameter distribution

Table 2 Experimental design matrix

Runs	Coded values			Response
	X_1 Mass dosage (g)	X_2 Caffeine initial concentration (mg/L)	X_3 pH	Y
1	(−) 0.10	(−) 20	(−) 2	81.88
3	(+) 0.20	(−) 20	(−) 2	95.85
5	(−) 0.10	(+) 80	(−) 2	42.93
7	(+) 0.20	(+) 80	(−) 2	70.32
9	(−) 0.10	(−) 20	(+) 10	74.99
11	(+) 0.20	(−) 20	(+) 10	85.98
10	(−) 0.10	(+) 80	(+) 10	37.27
8	(+) 0.20	(+) 80	(+) 10	58.12
6	(0) 0.15	(0) 50	(0) 6	65.30
4	(0) 0.15	(0) 50	(0) 6	62.49
2	(0) 0.15	(0) 50	(0) 6	60.51

RSM methodology

The effects of selected independent process variables were evaluated by the response surface methodology (RSM). Single and synergetic effects of 3 variables, i.e., X_1 adsorbent dosage (g), X_2 caffeine initial concentration (mg/L), and X_3 pH, were evaluated at 2 levels with the experimental response Y caffeine removal (Eq. 2). The total number of experiments of the 2^3 full experimental design was given as the sum of the $2^k + n_0$ (2^k, factorial runs; k, the number of independent process variables; and n_0, the center runs). Then, it was conducted 8 experiments + 8 duplicates + 3 central point runs, consisting of 19 experiments. The experimental levels of independent process variables are presented in Table 1. Equation 5 was used to predict the optimum condition of DS removal related to the interaction between dependent and independent variables. Besides, the analysis of variance (ANOVA) was used to validate the adequacy of model.

$$Y = b_0 + \sum_{i=1}^{n} b_i x_i + \sum_{i=1}^{n} b_{ii} x_i^2 + \sum_{i=1}^{n-1} \sum_{j=2}^{n} b_{ii} x_i x_j + \epsilon \quad (5)$$

Table 3 ANOVA

	Sum of squares	Degree of freedom	Mean of squares
Regression	30.15	5	6.03
Residues	0.81	13	0.06
Lack of fit	0.41	3	0.13
Pure error	35.79	10	0.03
$R^2 = 0.99$			

where Y is response; b_0 represents the intercept; b_{ij}, b_{ii}, and b_i are coefficients; n, number of variables; x_i and x_j, independent variables; and ε, the error (Kaynar et al. 2018).

Equilibrium studies

Equilibrium studies were performed using the contact time obtained in the kinetic studies, at 30, 40, 50, and 60 °C and DS concentrations of 50, 100, 200, 500, 750, and 1000 mg L^{-1}. The experimental data obtained were adjusted through the nonlinear regression using Langmuir (Eq. 6) (Langmuir 1918), Freundlich (Eq. 7) (Freundlich and Freundlich 1906, Redlich-Peterson (Eq. 8) (Redlich and Peterson 1959), and Sips (Eq. 9) (Sips 1948) models.

$$q_e = \frac{ce Q k_L}{1 + (ce k_L)} \quad (6)$$

$$q_e = k_F ce^{\frac{1}{n}} \quad (7)$$

$$q_e = \frac{ce k_{rp}}{\left(1 + a_{rp} ce^{b_{rp}}\right)} \quad (8)$$

$$q_e = \frac{q_S (k_S C_e)^{m_S}}{1 + (k_S C_e)^{m_S}} \quad (9)$$

where Q is the maximum adsorption capacity (mg g^{-1}); k_L is the Langmuir constant (L/mg); k_F is the Freundlich constant (mg g^{-1})(mg L^{-1})$^{-1/n}$; $1/n$ is the heterogeneity factor; k_{rp} (L

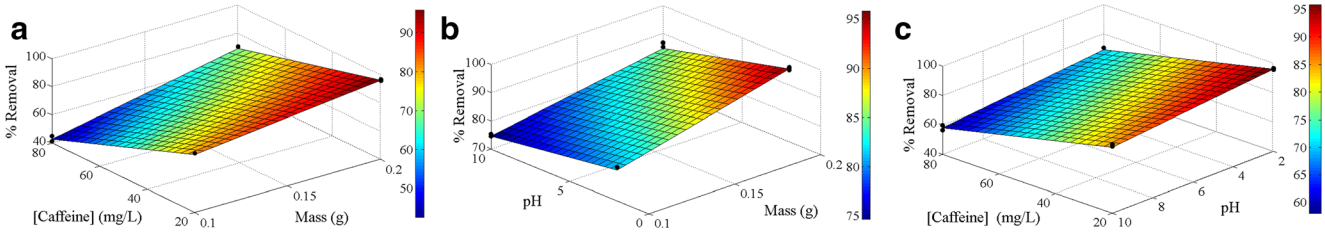

Fig. 5 Response surface plots

mg^{-1}), a_{rp} (L mg^{-1}), and β are Redlich-Peterson constants; q_S is the maximum adsorption capacity from the Sips model (mg g^{-1}); K_S is the Sips constant (L mg^{-1}); and m_S is the exponent of the Sips model.

In order to determine the accuracy of the models, the experimental data were evaluated using the correlation coefficient (R^2) and the relative mean error (ARE), presented in Eqs. 10 and 11, respectively (Piccin Jr et al. 2017).

$$R^2 = 1 - \frac{\sum_{i=1}^{n}\left(y_{i,exp} - y_{i,mod}\right)^2}{\sum_{i=1}^{n}\left(y_{i,exp} - \overline{y_{i,mod}}\right)^2} \quad (10)$$

$$ARE = \frac{100}{n}\sum_{i=1}^{n}\left|\frac{y_{i,exp} - y_{i,mod}}{y_{i,exp}}\right| \quad (11)$$

where y_{exp} is the value obtained experimentally, y_{mod} is the value predicted by the model, n_p is the number of parameters of the model, and n is the number of experimental points.

Adsorption assays using real matrixes

Tests were performed with real water samples, preparing solutions of 20 mg L^{-1} from tap, ultrapure, and mineral water. The parameters used were based on the previous study, 0.20 g of adsorbent, 25 mL of solution volume at 20 mg L^{-1} of caffeine initial concentration, 30 °C, pH 2, and 4 h. Samplings were performed in 15, 30, 45, 60, 120, 180, and 240 min, in duplicate. Solution concentration was determined by spectrophotometer UV-Vis (Shimadzu/UV-1800).

Results and discussions

Adsorbent characterization

The pH_{pzc} is obtained when the final pH is independent of initial pH (buffer effect) or when final pH is equal to initial pH. The pH_{pzc} indicates the pH at which the adsorbent has a net zero surface charge. The adsorbent has a positive charge when the solution pH is lower than the pH_{pzc}. On the other hand, when the solution pH is higher than the pH_{pzc}, the

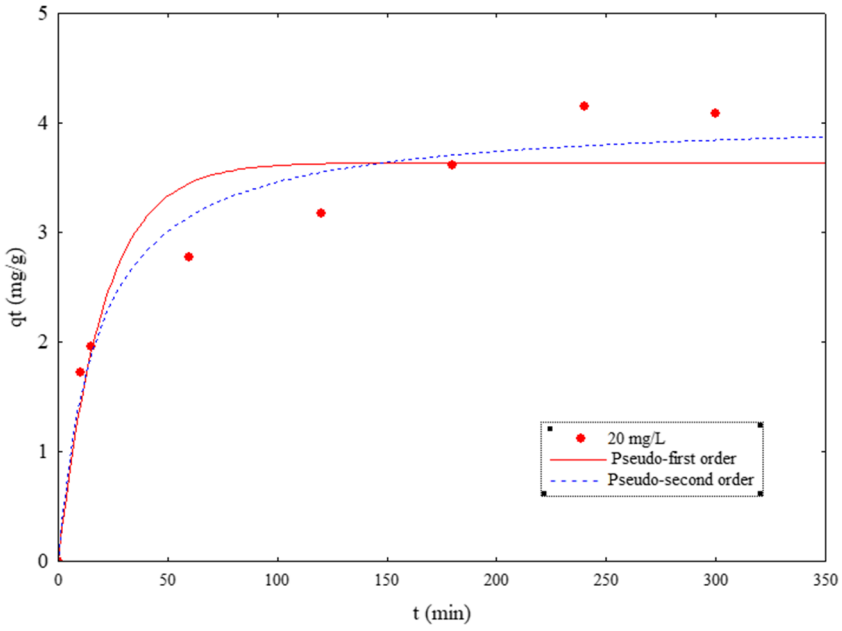

Fig. 6 Kinetic curve obtained for caffeine adsorption onto palm endocarp activated carbon and adjustments to pseudo-first-order and pseudo-second-order models

Table 4 Kinetic parameters obtained for the adjustment of the experimental data with pseudo-first-order and pseudo-second-order models

Pseudo-first-order				Pseudo-second-order			
R^2	q_e (mg/g)	ε (%)	K_f (min^{-1})	R^2	q_e (mg/g)	ε (%)	K (g/mg min)
0.91	3.64	11.87	0.04	0.96	4.07	8.77	0.01

adsorbent is negatively charged. Figure 1 depicts the result obtained for the activated carbon pH_{pzc} determination, in which the value obtained was around 6.3 (Kong et al. 2013).

The FT-IR spectrum, presented in Fig. 2, was obtained in the range of 4,000 to 400 cm^{-1}. The band between 3600 and 3200 cm^{-1}, with peak around 3461 cm^{-1}, is characteristic of group stretch vibrations -OH that may be related to the presence of hydroxyl and the water chemisorbed on carbon surface (Álvarez et al. 2015). The bands evidenced in 2956, 2924, 2850, 1425, and 460 cm^{-1} can be attributed to the presence of aliphatic groups, such as alkanes and alkenes, corresponding to C-H bonds (Sotelo et al. 2012; Álvarez et al. 2015). The band indicated in the region between 1650 and 1558 cm^{-1} is assigned to links C=C and C=O, present in carboxyl, carbonyl, and aromatic carbon radicals. Bands in 1425 and between 1118 and 1233 cm^{-1} are characteristics of phenolic and lactam groups (Fonts et al. 2009; Royer et al. 2009; Sotelo et al. 2012; Foletto et al. 2013; Larous and Meniai 2016).

SEM images at different magnifications are shown in Fig. 3. The activated carbon is a fine granular material confirming the diameters around 337.5 nm obtained by sieving. The material presented an irregular and heterogenic surface with the presence of pores, swellings, and canals. These characteristics are propitious for adsorption since the interaction between liquid and solid may occur in the internal and external surfaces (Georgin et al. 2019).

N_2 adsorption/desorption isotherm presented in Fig. 4 a may be classified as type IV according to IUPAC (Thommes et al. 2015). This type of isotherm is characteristic of mesoporous materials with an evident hysteresis, due to increased pressure that causes an increase in the volume of N_2 adsorbed

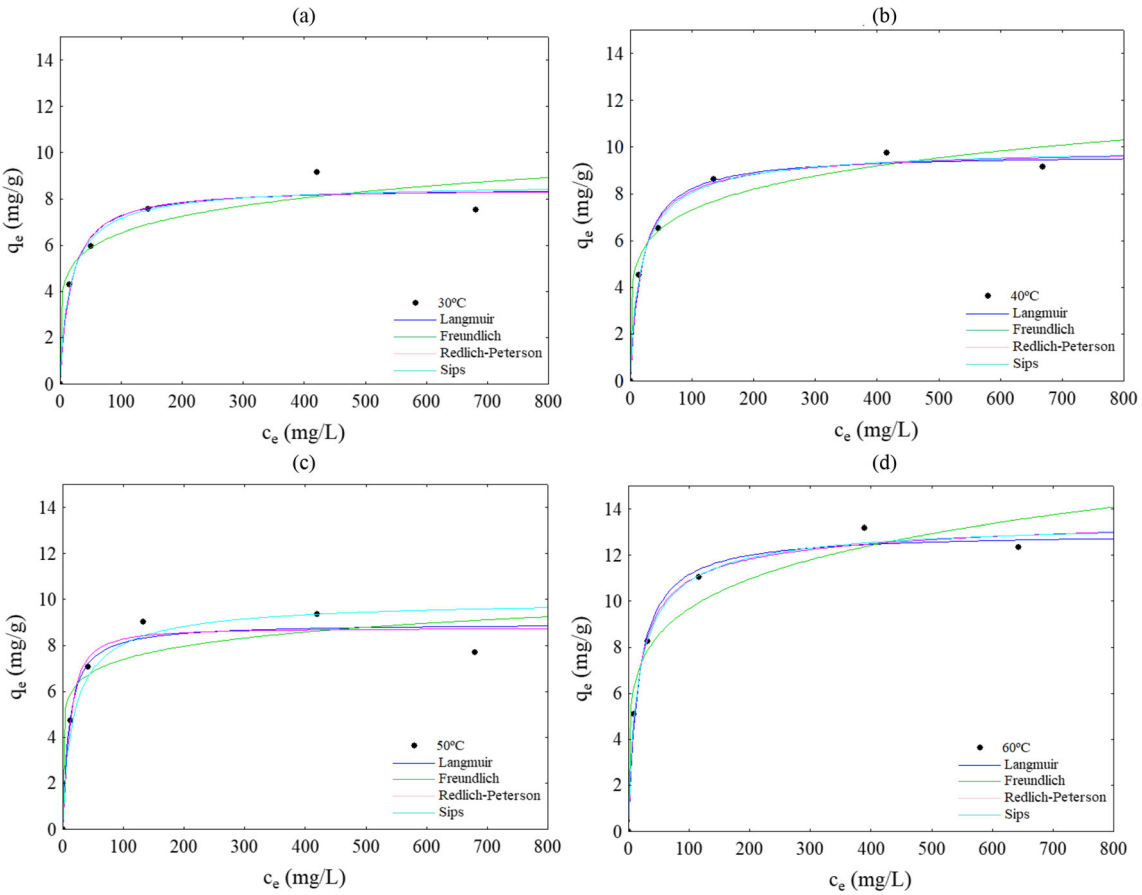

Fig. 7 Isotherms obtained for caffeine adsorption onto palm endocarp activated carbon at 30 °C (**a**), 40 °C (**b**), 50 °C (**c**), and 60 °C (**d**) and adjustments to Langmuir, Freundlich, Redlich-Peterson, and Sips models

Table 5 Equilibrium parameters obtained for the adjustment of the experimental data with Langmuir, Freundlich, Redlich-Peterson, and Sips models

Models	Parameters	30 °C	40 °C	50 °C	60 °C
Langmuir	Q (mg g^{-1})	8.501	9.714	8.952	12.982
	K_L (L mg^{-1})	0.058	0.055	0.098	0.061
	R^2	0.967	0.991	0.965	0.977
	ARE	6.670	4.400	6.560	6.450
Freundlich	K_F [(mg L^{-1})(L g^{-1})$^{1/n}$]	3.271	3.405	4.497	4.215
	n	6.660	6.032	9.275	5.541
	R^2	0.937	0.965	0.904	0.890
	ARE	10.390	8.660	14.070	10.710
Redlich-Peterson	K_{rp} (L mg^{-1})	0.484	0.590	0.557	0.933
	A_{rp} (L mg^{-1})$^{\beta}$	0.055	0.069	0.034	0.089
	β	1.005	0.980	1.099	0.966
	R^2	0.967	0.992	0.978	0.981
	ARE	6.320	4.230	6.460	3.380
Sips	q_s (mg g^{-1})	8.714	10.073	8.750	13.582
	K_S (L mg^{-1})	0.085	0.087	0.045	0.098
	m_S	0.866	0.829	1.291	0.806
	R^2	0.968	0.993	0.968	0.984
	ARE	6.000	3.610	6.760	2.490

(Beltrame et al. 2018). In addition, the desorption process presents a very marked and open hysteresis, indicating the occurrence of a sudden nitrogen desorption or its enclosure in the material pores, and a gas condensation may occur, something common in mesoporous materials (Zhang et al. 2015). According to the distribution of mesoporous sizes in Fig. 4 b, varying from 21 to 40 Å (2.50–4.0 nm), with an average diameter of 30.51 Å. Macroporous sizes appear in the range of 90 to 130 Å (9.0–13.0 nm) and 220 to 320 Å (22.0–32.0 nm). In addition, the material presented a specific area of 407.66 m^2 g^{-1} and total pore volume of 0.169 cm^3 g^{-1}. Ferreira et al. (2015) obtained different values, 672 m^2 g^{-1} and 0.369 cm^3 g^{-1}, for *dendê* mesocarp activated carbon, which considering the variability of climate, soil, harvest, and other agricultural characteristics, it is totally expected.

RSM analysis

The final experimental design matrix for the three independent variables with response is presented in Table 2. The experimental mathematical model in terms of coded variables and with more significant coefficients is presented by Eq. 12.

$$Y = \underset{(\pm 0{,}570)}{67{,}748} + \underset{(\pm 0{,}669)}{9{,}149}\,X_1 - \underset{(\pm 0{,}669)}{16{,}258}\,X_2 - \underset{(\pm 0{,}669)}{4{,}330}\,X_3 - \underset{(\pm 0{,}669)}{2{,}909}\,X_1X_2 \quad (12)$$

Table 6 Comparison between the activated carbon obtained from *Elaeis guineensis* endocarp and other materials for caffeine removal

Adsorbent	Maximum adsorption capacity (mg g^{-1})	References
Activated carbon obtained from *Elaeis guineensis* endocarp	13.582	This work
Carbon fibers prepared from pineapple leaves	152.18	Beltrame et al. (2018)
Carbon nanotubes	4.18	Gil et al. (2018)
Carbon xerogels	182.5	Álvarez et al. (2015)
Oxidized biochar from pine needles	6.54	Anastopoulos et al. (2020)
MgAl-LDH/biochar composite	26.219	dos Santos Lins et al. (2019)
Oxidized carbon derived from *Luffa cylindrica*	59.88	Ramirez et al. (2020)

Table 7 Thermodynamic parameters obtained for caffeine adsorption onto palm endocarp activated carbon

Temperature (°C)	$\Delta G°$ (kJ/mol)	$\Delta H°$ (kJ/mol)	$\Delta S°$ (kJ/mol)
30	− 17.190	− 1.553	0.0508
40	− 17.818		
50	− 16.615		
60	− 19.285		

Analysis of variance (ANOVA) of mathematical/statistical model is shown in Table 3. The model was statistically significant since R^2 was high and values of lack of fit and pure error were low indicating the model can predict successfully the experimental data. F test showed calculated F (96.33) was higher than the standard F (3.03); besides, the ration between calculated F and standard F was higher than 1.0 ($F_{calculated}/F_{standard}$ = 31.79) confirming the model validation.

The response surface plots are presented in Fig. 5. Figure 5 a shows the effect of caffeine initial concentration and mass dosage on the percentage of removal. Removal increases with the decrease of concentration and increase of pH. In Fig. 5 b is presented the influence of pH and mass of adsorbent on the removal of caffeine. Removal increases with the augment of mass dosage; however, it is not observed a significant influence of pH. A similar behavior is observed in Fig. 5 c where the caffeine initial concentration had a more significant effect on the caffeine removal than pH. The augmentation of adsorbate concentration is proportional to the increase in the number of molecules in the medium competing for the available active sites on the adsorbent surface. When the adsorbent surface is saturated by adsorbates, the caffeine molecules remain in solution. The increase in dosage provides an increase in the removal. However, this direct relation is intimately linked with caffeine concentration and pH, since for low amounts of adsorbate, it was obtained high values of removal (> 74.55%). pH was the parameter with the lowest influence; the highest values of removal were obtained in acid medium. When the solution pH is higher than the pH_{pzc} the adsorbent is negatively charged. In this condition, the caffeine is attracted by the adsorbent surface since they have opposite charges (Couto et al. 2015).

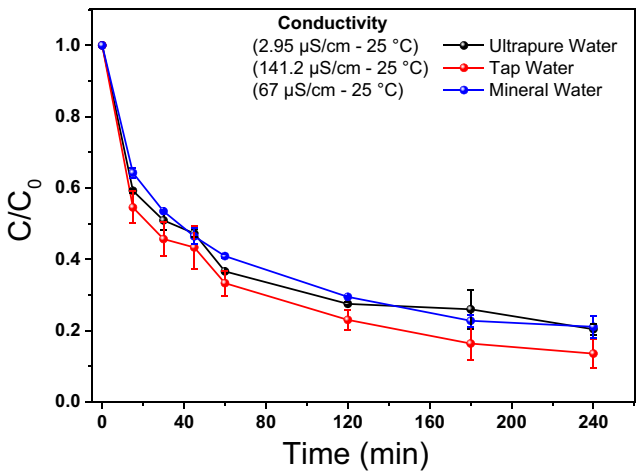

Fig. 8 Adsorption in real matrixes

Kinetic study

Kinetic studies are fundamental to better understand the adsorption mechanisms involved as well as to evaluate the efficiency of the separation process. Assays performed from 5 to 300 min of contact between adsorbent and adsorbate (20 mg/L) showed that the equilibrium of caffeine adsorption onto palm endocarp activated carbon was reached after 5 h. Figure 6 shows the kinetic curve and the adjustment of the experimental data with the pseudo-first-order and pseudo-second-order models. The statistic parameters are presented in Table 4. According to the results obtained, the experimental data fitted better with the pseudo-secondo-order model, due to the higher determination coefficient (R^2 = 0.96) and lower error (ARE = 8.77), when compared with the pseudo-first-order parameters (R^2 = 0.91 and ARE = 11.87). It suggests that chemisorption is the dominant adsorption mechanisms involved, justifying the slow kinetics observed.

Equilibrium studies

Isotherm curves were performed at 30, 40, 50, and 60 °C in order to evaluate the type of interaction between the adsorbent and the adsorbate. The experimental data, as well as the adjustments for Langmuir, Freundlich, Redlich-Peterson, and Sips models, are depicted in Fig. 7. The parameters obtained are shown in Table 5. From the results achieved, the temperature increase favored the adsorption, indicating an exothermic process for caffeine concentrations up to 500 mg/L, reaching the adsorptive capacity of 13.17 mg/g. However, for all isotherms, adsorption decreased when the initial adsorbate concentration was 750 mg/L. This result can be explained by saturation of adsorbent which, when the equilibrium was reached at 500 mg L^{-1}, almost all active sites are occupied, reducing the removal of the dispersed molecules, decreasing adsorption efficiency.

Among all models, Redlich-Peterson and Sips were the ones who presented the best fit to the experimental data, based on the highest R^2 values and the lowest ARE. Once both isotherms are hybrids of Langmuir and Freundlich's models, they can overcome some limitations of the two parameter models. Therefore, in general, experimental data fitted better to the Sips model, presenting higher coefficient of determination (R^2) and lower average relative error (ARE), predicting a maximum adsorption capacity of 13.5 mg g^{-1}, closed to the experimental value. The isotherm profile indicates they can be

classified as L-2 type, according Giles et al. (1960). It is evident a marked initial rise and a concavity in relation to the *x*-axis at low equilibrium concentration. This result is characteristic of systems in which the adsorbate has a strong affinity with adsorbent, and there is no significant competition of the solvent for active sites, allowing the formation of a monolayer on the surface (Gil et al. 2018). Besides, this type of isotherm indicates that more solute loading can be carried into the solid, as long as it is at lower concentrations (Couto et al. 2015).

In order to compare the effectiveness of activated carbon obtained from *Elaeis guineensis* endocarp in the removal of caffeine from aqueous solution, in Table 6 is presented a comparison between the maximum adsorption capacities (q_m) of different adsorbents. Activated carbon obtained from *Elaeis guineensis* endocarp seems to be a promising material for caffeine removal since it presents q_m values similar with other activated carbons as well as much more complex materials such nanotubes and composites.

Thermodynamic studies

Thermodynamics studies are important to understand the mechanism, spontaneity, and nature of adsorption and the adsorbent surface characteristics. Considering that the Sips model presented the best fit to the experimental data, K_s, the equilibrium thermodynamic constant, was used to calculate ΔG^0 for all temperatures studied using Eq. 13. Then, by the plot of ln (K_s) versus ($1/T$), van't Hoff plot, the values of ΔH^0 and ΔS^0 were found. Table 7 summarizes the thermodynamic parameters (ΔG^0, ΔH^0, and ΔS^0) obtained.

$$\Delta G^0 = -RTlnK_s \tag{13}$$

where R is the universal gas constant (8.314 J mol^{-1} K^{-1}), T is the temperature (K), and K_s is the thermodynamic equilibrium constant.

From the data obtained, the negative values of ΔG^0 indicate that adsorption was spontaneous at all temperatures studied. In addition, more negative values are obtained with higher temperatures indicating adsorption is favored by temperature. By analyzing the ΔH^0, the negative value indicates the process was exothermic; this behavior is related to the desolvation of water molecules from the solid surface for adsorption of caffeine molecules. The enthalpy value between 0 and − 40 kJ mol^{-1} presupposes a physisorption phenomenon. According to the positive S^0, possibly some structural changes or readjustments in the adsorbate-adsorbent complex occurred demonstrating that the interaction is entropy-controlled (Silva et al. 2017; Lütke et al. 2019; Meili et al. 2019; dos Santos Lins et al. 2019). Similar results were obtained by Beltrame et al. (2018) and Anastopoulos and Pashalidis (2019), using activated carbon fibers from pineapple leaves and oxidized activated carbon derived from *Luffa cylindrica* for caffeine removal, respectively.

Adsorption in real water matrixes

Figure 8 shows the results of caffeine concentration behavior versus time according to the aqueous matrix. A higher percentage (98.54%) of caffeine removal was obtained using tap water, with lower and similar percentages for ultrapure water (91.64%) and mineral water (91.30%). In the tap water, several dissolved anions, such as sulfate and chloride, from water treatment process, may have interacted, electrostatically, with caffeine molecules, leaving it with an opposite load in relation with carbon surface, favoring the adsorption. This characteristic may be proven by the conductivity of water matrixes (Wu et al. 2020). Although mineral water presented higher conductivity than ultrapure water, dissolved anions presented milder action. Satisfactory results indicate that palm endocarp activated carbon has a high potential to treat the water contaminated with caffeine.

Conclusions

The present contribution demonstrated the feasibility of using the palm endocarp activated carbon for caffeine removal from water. Assays performed through a complete experimental design 2^3 showed that the most significant tested parameter was adsorbate concentration, followed by mass of adsorbent and solution pH. The best response was achieved using 0.20 g of adsorbent, initial caffeine concentration of 20 mg/L, and pH 2, reaching a total removal of 95.8%. From the kinetic studies, equilibrium was attained after 5 h and the experimental data presented the best fit to the pseudo-second-order model, suggesting chemisorption as the predominant adsorption mechanism. The isotherms studies provided best fit to the Redlich-Peterson and Sips (adsorption capacity of 13.5 mg/g) models. Finally, thermodynamics calculations indicated an exothermic and spontaneous adsorption mechanism with structural modifications in the adsorbate-adsorbent interface. The positive results obtained regarding adsorption in different water matrixes demonstrated the ability to be used as an adsorbent agent in complex conditions. The adsorbent features and efficient removal results suggest a suitable material for caffeine withdrawn from water.

Acknowledgments The authors thank Conselho Nacional de Desenvolvimento Científico e Tecnológico (CNPq/Brazil), Coordenação de Aperfeiçoamento de Pessoal de Nível Superior (CAPES/Brazil), and Fundação de Amparo à Pesquisa do Estado de Alagoas (FAPEAL/Brazil).

References

Abatan OG, Oni BA, Agboola O, Efevbokhan V, Abiodun OO (2019) Production of activated carbon from African star apple seed husks, oil seed and whole seed for wastewater treatment. J Clean Prod 232: 441–450. https://doi.org/10.1016/j.jclepro.2019.05.378

Álvarez S, Ribeiro RS, Gomes HT, Sotelo JL, García J (2015) Synthesis of carbon xerogels and their application in adsorption studies of caffeine and diclofenac as emerging contaminants. Chem Eng Res Des 95:229–238. https://doi.org/10.1016/j.cherd.2014.11.001

Álvarez-Torrellas S, Sotelo JL, Rodríguez A, Ovejero G, García J (2017) Influence of the natural organic matter in the removal of caffeine from water by fixed-bed column adsorption. Int J Environ Sci Technol 14:833–840. https://doi.org/10.1007/s13762-016-1189-7

Anastopoulos I, Pashalidis I (2019) The application of oxidized carbon derived from Luffa cylindrica for caffeine removal. Equilibrium, thermodynamic, kinetic and mechanistic analysis. J Mol Liq 296: 112078. https://doi.org/10.1016/j.molliq.2019.112078

Anastopoulos I, Katsouromalli A, Pashalidis I (2020) Oxidized biochar obtained from pine needles as novel adsorbent to remove caffeine from aqueous solutions. J Mol Liq 304:112661. https://doi.org/10.1016/j.molliq.2020.112661

Barsç S, Turkay O (2016) Optimization and modelling using the response surface methodology (RSM) for ciprofloxacin removal by electrocoagulation. Water Sci Technol 73:1673–1679. https://doi.org/10.2166/wst.2015.649

Beltrame KK, Cazetta AL, de Souza PSC, Spessato L, Silva TL, Almeida VC (2018) Adsorption of caffeine on mesoporous activated carbon fibers prepared from pineapple plant leaves. Ecotoxicol Environ Saf 147:64–71. https://doi.org/10.1016/j.ecoenv.2017.08.034

Biswas S, Bal M, Behera SK, Sen T, Meikap B (2019) Process optimization study of Zn 2+ + adsorption on biochar-alginate composite adsorbent by response surface methodology (RSM). Water (Switzerland) 11. https://doi.org/10.3390/w11020325

Chandana L, Krushnamurty K, Suryakala D, Subrahmanyam C (2019) Low-cost adsorbent derived from the coconut shell for the removal of hexavalent chromium from aqueous medium. Mater Today Proc. https://doi.org/10.1016/j.matpr.2019.04.205

Couto OM, Matos I, da Fonseca IM et al (2015) Effect of solution pH and influence of water hardness on caffeine adsorption onto activated carbons. Can J Chem Eng 93:68–77. https://doi.org/10.1002/cjce.22104

Darvishmotevalli M, Zarei A, Moradnia M, Noorisepehr M, Mohammadi H (2019) Optimization of saline wastewater treatment using electrochemical oxidation process: prediction by RSM method. MethodsX 6:1101–1113. https://doi.org/10.1016/j.mex.2019.03.015

De Azevedo EG, Follegatti-romero LA, Duvoisin S, Aznar M (2014) Liquid – liquid equilibria for ternary systems containing ethylic palm oil biodiesel + ethanol + glycerol / water: experimental data at 298.15 and 323.15 K and thermodynamic modeling. Fuel 128: 356–365. https://doi.org/10.1016/j.fuel.2014.01.074

Deng S, Chen Y (2019) A study by response surface methodology (RSM) on optimization of phosphorus adsorption with nano spherical calcium carbonate derived from waste. Water Sci Technol 79:188–197. https://doi.org/10.2166/wst.2019.048

Deveci EÜ, Akarsu C, Gönen Ç, Özay Y (2019) Enhancing treatability of tannery wastewater by integrated process of electrocoagulation and fungal via using RSM in an economic perspective. Process Biochem 84:124–133. https://doi.org/10.1016/j.procbio.2019.06.016

Domínguez JR, González T, Palo P et al (2016) Conductive-diamond electrochemical oxidation of a pharmaceutical effluent with high chemical oxygen demand (COD). Kinetics and optimization of the process by response surface methodology (RSM). Environ Eng Manag J 15:27–34. https://doi.org/10.30638/eemj.2016.004

dos Santos Lins PV, Henrique DC, Ide AH, de Paiva e Silva Zanta CL, Meili L (2019) Evaluation of caffeine adsorption by MgAl-LDH/biochar composite. Environ Sci Pollut Res 26:31804–31811. https://doi.org/10.1007/s11356-019-06288-3

dos Santos KJL, de Souza dos Santos GE, de Sá ÍMGL, de Carvalho SHV, Soletti JI, Meili L, da Silva Duarte JL, Bispo MD, Dotto GL (2019a) Syagrus oleracea–activated carbon prepared by vacuum pyrolysis for methylene blue adsorption. Environ Sci Pollut Res 26: 16470–16481. https://doi.org/10.1007/s11356-019-05083-4

dos Santos KJL, de Suoza dos Santos GE, de Sá ÍMGL et al (2019b) Wodyetia bifurcata biochar for methylene blue removal from aqueous matrix. Bioresour Technol 293:122093. https://doi.org/10.1016/j.biortech.2019.122093

Duarte JLS, Meili L, Gomes LM, Melo JMO, Ferro AB, Tavares MG, Tonholo J, Zanta CLPS (2019) Electrochemical degradation of 17-A-methyltestosterone over DSA® electrodes. Chem Eng Process Process Intensif 142:107548. https://doi.org/10.1016/j.cep.2019.107548

Ferreira RC, Couto Junior OM, Carvalho KQ et al (2015) Effect of solution pH on the removal of Paracetamol by activated carbon of dende coconut mesocarp. Chem Biochem Eng Q J 29:47–53. https://doi.org/10.15255/cabeq.2014.2115

Foletto EL, Weber CT, Paz DS, Mazutti MA, Meili L, Bassaco MM, Collazzo GC (2013) Adsorption of leather dye onto activated carbon prepared from bottle gourd: equilibrium, kinetic and mechanism studies. Water Sci Technol 67:201–209. https://doi.org/10.2166/wst.2012.555

Fonts I, Azuara M, Gea G, Murillo MB (2009) Study of the pyrolysis liquids obtained from different sewage sludge. J Anal Appl Pyrolysis 85:184–191. https://doi.org/10.1016/j.jaap.2008.11.003

Freundlich H, Freundlich HMF (1906) Over the adsorption in solution. J Phys Chem 57:358–471

Galedari M, Mehdipour Ghazi M, Rashid Mirmasoomi S (2019) Photocatalytic process for the tetracycline removal under visible light: presenting a degradation model and optimization using response surface methodology (RSM). Chem Eng Res Des 145: 323–333. https://doi.org/10.1016/j.cherd.2019.03.031

Garg KK, Prasad B (2015) Electrochemical treatment of benzoic acid (BA) from aqueous solution and optimization of parameters by response surface methodology (RSM). J Taiwan Inst Chem Eng 56: 122–130. https://doi.org/10.1016/j.jtice.2015.04.005

Georgin J, Franco DSP, Grassi P, Tonato D, Piccilli DGA, Meili L, Dotto GL (2019) Potential of Cedrella fissilis bark as an adsorbent for the removal of red 97 dye from aqueous effluents. Environ Sci Pollut Res 26:19207–19219. https://doi.org/10.1007/s11356-019-05321-9

Gil A, Santamaría L, Korili SA (2018) Removal of caffeine and diclofenac from aqueous solution by adsorption on multiwalled carbon nanotubes. Colloids Interface Sci Commun 22:25–28. https://doi.org/10.1016/j.colcom.2017.11.007

Giles CH, Macewan TH, Nakhwa SN, Smith D (1960) Studies in adsorption. Part XI. A system of classification of solution adsorption isotherms, and it use in diagnosis of adsorption mechanisms and in measurement of specific surface areas of solids. J Chem Soc 111: 3973–3993

González VR, Escobedo-Morales A, Cortés-Arriagada D, Ruiz Peralta ML, Anota EC (2019) Enhancement of caffeine adsorption on boron nitride fullerene by silicon doping. Appl Nanosci 9:317–326. https://doi.org/10.1007/s13204-018-0901-y

Hasan R, Setiabudi HD (2019) Removal of Pb(II) from aqueous solution using KCC-1: optimization by response surface methodology (RSM). J King Saud Univ Sci 31:1182–1188. https://doi.org/10.1016/j.jksus.2018.10.005

Ho YS, McKay G (1999) Pseudo-second order model for sorption processes. Process Biochem 34:451–465. https://doi.org/10.1016/S0032-9592(98)00112-5

Karamati-Niaragh E, Alavi Moghaddam MR, Emamjomeh MM, Nazlabadi E (2019) Evaluation of direct and alternating current on nitrate removal using a continuous electrocoagulation process: economical and environmental approaches through RSM. J Environ Manag 230:245–254. https://doi.org/10.1016/j.jenvman.2018.09.091

Karimi P, Baneshi MM, Malakootian M (2019) Photocatalytic degradation of aspirin from aqueous solutions using the UV/ZnO process: modelling, analysis and optimization by response surface methodology (RSM). Desalin Water Treat 161:354–364. https://doi.org/10.5004/dwt.2019.24317

Kaur I, Gupta A, Singh BP, Kumar R, Chawla J (2019) Defluoridation of water using micelle templated MCM-41: adsorption and RSM studies. J Water Supply Res Technol AQUA 68:282–294. https://doi.org/10.2166/aqua.2019.013

Kaynar ÜH, Çınar S, Çam Kaynar S, Ayvacıklı M, Aydemir T (2018) Modelling and optimization of uranium (VI) ions adsorption onto nano-ZnO/chitosan bio-composite beads with response surface methodology (RSM). J Polym Environ 26:2300–2310. https://doi.org/10.1007/s10924-017-1125-z

Kong L, Gong L, Wang J (2013) Removal of methylene blue from wastewater using fallen leaves as an adsorbent. Desalin Water Treat 53:1–12. https://doi.org/10.1080/19443994.2013.863738

Lagergren S (1898) About the theory of so-called adsorption of soluble substances. K Sven Vetenskapsakademiens 24:1–39

Langmuir I (1918) The adsorption of gases on plane surfaces of glass, mica and platinum. J Am Chem Soc 40:1361–1403. https://doi.org/10.1021/ja02242a004

Larous S, Meniai A-H (2016) Adsorption of diclofenac from aqueous solution using activated carbon prepared from olive stones. Int J Hydrog Energy 41:10380–10390. https://doi.org/10.1016/j.ijhydene.2016.01.096

Liu D, Gu G, Wu B, Wang C, Chen X (2018) Degradation of isopropyl ethylthionocarbamate from aqueous solution by fenton oxidation: RSM optimization, mechanisms, and kinetic analysis. Desalin Water Treat 130:87–97. https://doi.org/10.5004/dwt.2018.22846

Lütke SF, Igansi AV, Pegoraro L, Dotto GL, Pinto LAA, Cadaval TRS Jr (2019) Preparation of activated carbon from black wattle bark waste and its application for phenol adsorption. J Environ Chem Eng 7:103396. https://doi.org/10.1016/j.jece.2019.103396

Lv S, Li C, Mi J, Meng H (2020) A functional activated carbon for efficient adsorption of phenol derived from pyrolysis of rice husk, KOH-activation and EDTA-4Na-modification. Appl Surf Sci 510:145425. https://doi.org/10.1016/j.apsusc.2020.145425

Meili L, Godoy RPS, Soletti JI, Carvalho SHV, Ribeiro LMO, Silva MGC, Vieira MGA, Gimenes ML (2019) Cassava (Manihot esculenta Crantz) stump biochar: physical/chemical characteristics and dye affinity. Chem Eng Commun 206:829–841. https://doi.org/10.1080/00986445.2018.1530991

Mirzaei M, Sabbaghi S, Zerafat MM (2018) Photo-catalytic degradation of formaldehyde using nitrogen-doped TiO2 nano-photocatalyst: statistical design with response surface methodology (RSM). Can J Chem Eng 96:2544–2552. https://doi.org/10.1002/cjce.23192

Murdani J, Ekawati D et al (2018) Application of response surface methodology (RSM) for wastewater of hospital by using electrocoagulation. IOP Conf Ser Mater Sci Eng 345:012011. https://doi.org/10.1088/1757-899X/345/1/012011

Piccin JS Jr, Cadaval TRSA Jr, de Pinto LAA, Dotto GL (2017) Adsorption isotherms in liquid phase: experimental, modeling, and interpretations. In: Bonilla-Petriciolet A, Mendoza-Castillo DI, Reynel-Avila HE (eds) Adsorption processes for water treatment, pp 19–51

Portinho R, Zanella O, Féris LA (2017) Grape stalk application for caffeine removal through adsorption. J Environ Manag 202:178–187. https://doi.org/10.1016/j.jenvman.2017.07.033

Ptaszkowska-Koniarz M, Goscianska J, Pietrzak R (2018) Synthesis of carbon xerogels modified with amine groups and copper for efficient adsorption of caffeine. Chem Eng J 345:13–21. https://doi.org/10.1016/j.cej.2018.03.132

Queiroz AG, França L, Ponte MX (2012) The life cycle assessment of biodiesel from palm oil (“ dendê”) in the Amazon. Biomass Bioenergy 36:50–59. https://doi.org/10.1016/j.biombioe.2011.10.007

Rabahi A, Hauchard D, Arris S, Berkani M, Achouri O, Meniai AH, Bencheikh-Lehocine M (2018) Leachate effluent COD removal using electrocoagulation: a response surface methodology (RSM) optimization and modelling. Desalin Water Treat 114:1–12. https://doi.org/10.5004/dwt.2018.22318

Ramirez A, Ocampo R, Giraldo S, Padilla E, Flórez E, Acelas N (2020) Removal of Cr (VI) from an aqueous solution using an activated carbon obtained from teakwood sawdust: kinetics, equilibrium, and density functional theory calculations. J Environ Chem Eng 8:103702. https://doi.org/10.1016/j.jece.2020.103702

Redlich O, Peterson DL (1959) A useful adsorption isotherm. J Phys Chem 63:1024

Regalbuto J (2006) Catalyst preparation: Science and Engineering. CRC Press, Boca Raton

Royer B, Cardoso NF, Lima EC, Vaghetti JCP, Simon NM, Calvete T, Veses RC (2009) Applications of Brazilian pine-fruit shell in natural and carbonized forms as adsorbents to removal of methylene blue from aqueous solutions-kinetic and equilibrium study. J Hazard Mater 164:1213–1222. https://doi.org/10.1016/j.jhazmat.2008.09.028

Saeed MO, Azizli K, Isa MH, Bashir MJK (2015) Application of CCD in RSM to obtain optimize treatment of POME using Fenton oxidation process. J Water Process Eng 8:e7–e16. https://doi.org/10.1016/j.jwpe.2014.11.001

Şahan T (2019) Application of RSM for Pb(II) and Cu(II) adsorption by bentonite enriched with [sbnd]SH groups and a binary system study. J Water Process Eng 31:100867. https://doi.org/10.1016/j.jwpe.2019.100867

Sharifpour E, Alipanahpour Dil E, Asfaram A, Ghaedi M, Goudarzi A (2019) Optimizing adsorptive removal of malachite green and methyl orange dyes from simulated wastewater by Mn-doped CuO-nanoparticles loaded on activated carbon using CCD-RSM: mechanism, regeneration, isotherm, kinetic, and thermodynamic studies. Appl Organomet Chem 33:1–14. https://doi.org/10.1002/aoc.4768

Silva TS, Meili L, Carvalho SHV, Soletti JI, Dotto GL, Fonseca EJS (2017) Kinetics, isotherm, and thermodynamic studies of methylene blue adsorption from water by Mytella falcata waste. Environ Sci Pollut Res 24:19927–19937. https://doi.org/10.1007/s11356-017-9645-6

Sips R (1948) On the structure of a catalyst surface. J Phys Chem 16:490–495. https://doi.org/10.1063/1.1746922

Sotelo JL, Rodriguez A, Alvarez S, Garcia J (2012) Removal of caffeine and diclofenac on activated carbon in fixed bed column. Chem Eng Res Des 90:967–974. https://doi.org/10.1016/j.cherd.2011.10.012

Suzuki RM, Andrade AD, Sousa JC, Rollemberg MC (2007) Preparation and characterization of activated carbon from rice bran. Bioresour Technol 98:1985–1991. https://doi.org/10.1016/j.biortech.2006.08.001

Thommes M, Kaneko K, Neimark AV, Olivier JP, Rodriguez-Reinoso F, Rouquerol J, Sing KSW (2015) Physisorption of gases, with special reference to the evaluation of surface area and pore size distribution (IUPAC Technical Report). Pure Appl Chem 87:1051–1069. https://doi.org/10.1515/pac-2014-1117

Thorn CF, Aklillu E, McDonagh EM et al (2012) PharmGKB summary: caffeine pathway. Pharmacogenet Genomics 22:389–395. https://doi.org/10.1097/FPC.0b013e3283505d5e

Wakkel M, Khiari B, Zagrouba F (2019) Basic red 2 and methyl violet adsorption by date pits: adsorbent characterization, optimization by

RSM and CCD, equilibrium and kinetic studies. Environ Sci Pollut Res 26:18942–18960. https://doi.org/10.1007/s11356-018-2192-y

Wang J, Sun Y, Jiang H, Feng J (2017) Removal of caffeine from water by combining dielectric barrier discharge (DBD) plasma with goethite. J Saudi Chem Soc 21:545–557. https://doi.org/10.1016/j.jscs.2016.08.002

Weber CT, Foletto EL, Meili L (2013) Removal of tannery dye from aqueous solution using papaya seed as an efficient natural biosorbent. Water Air Soil Pollut 224. https://doi.org/10.1007/s11270-012-1427-7

Wu Y, Wang F, Jin X, Zheng X, Wang Y, Wei D, Zhang Q, Feng Y, Xie Z, Chen P, Liu H, Liu G (2020) Highly active metal-free carbon dots/g-C3N4 hollow porous nanospheres for solar-light-driven PPCPs remediation: mechanism insights, kinetics and effects of natural water matrices. Water Res 172:115492. https://doi.org/10.1016/j.watres.2020.115492

Xie Y, Chen L, Liu R (2016) Oxidation of AOX and organic compounds in pharmaceutical wastewater in RSM-optimized-Fenton system. Chemosphere 155:217–224. https://doi.org/10.1016/j.chemosphere.2016.04.057

Yamamoto K, Shiono T, Yoshimura R, Matsui Y, Yoneda M (2018) Influence of hydrophilicity on adsorption of caffeine onto montmorillonite. Adsorpt Sci Technol 36:967–981. https://doi.org/10.1177/0263617417735480

Zhang H, Liu X, He G, Zhang X, Bao S, Hu W (2015) Bioinspired synthesis of nitrogen/sulfur co-doped graphene as an efficient electrocatalyst for oxygen reduction reaction. J Power Sources 279:252–258. https://doi.org/10.1016/j.jpowsour.2015.01.016